EFDA–JET–PR(09)21

A. Murari, M. Camplani, B. Cannas, D. Mazon, F.Delaunay, P.Usai,
J.F.Delmond and JET EFDA contributors

Algorithms for the Automatic Identification of MARFEs and UFOs in JET Database of Visible Camera Videos

Algorithms for the Automatic Identification of MARFEs and UFOs in JET Database of Visible Camera Videos

A. Murari[1], M. Camplani[2], B. Cannas[2], D. Mazon[3], F. Delaunay[4], P. Usai[2],
J.F. Delmond[4] and JET EFDA contributors*

JET-EFDA, Culham Science Centre, OX14 3DB, Abingdon, UK

[1]Consorzio RFX-Associazione EURATOM ENEA per la Fusione, I-35127 Padova, Italy.
[2]Electrical and Electronic Engineering Department, University of Cagliari, Cagliari, Italy
[3]Association EURATOM-CEA, CEA Cadarache DSM/IRFM, 13108 Saint-Paul-lez-Durance, France
[4]Arts et Métiers ParisTech Engineering College (ENSAM) 75013 Paris
** See annex of F. Romanelli et al, "Overview of JET Results",*
(Proc. 22 [nd] IAEA Fusion Energy Conference, Geneva, Switzerland (2008)).

Preprint of Paper to be submitted for publication in
IEEE Transactions on Plasma Science

ABSTRACT.
MARFE instabilities and UFOs leave clear signatures in JET fast visible camera videos. Given the potential harmful consequences of these events, particularly as triggers of disruptions, it would be important to have means of detecting them automatically. In this paper, the results of various algorithms to identify automatically MARFEs and UFOs in JET visible videos are reported. The objective is to retrieve videos, which have captured these events, exploring the whole JET database of images, as a preliminary step to the development of real time identifiers in the future. For the detection of MARFEs, a complete identifier has been finalized, using morphological operators and Hu moments. The final algorithm manages to identify videos with MARFEs with a success rate exceeding 80%. Due to lack of a complete statistics of examples, the UFO identifier is less developed but a preliminary code can detect UFOs quite reliably.

1. INTRODUCTION

In the last decades the technology of cameras has improved dramatically. Particularly relevant for scientific applications is the availability of reliable and very performing digital cameras. Their versatility and potential has strongly contributed to their widespread use as diagnostics for nuclear fusion. In JET for example [1], cameras are becoming more common for both scientific and surveying applications. On the other hand, since these technologies are relatively new in the diagnostic sets of present day Tokamaks, the information present in the videos is not always fully exploited. In particular, since some of the most advanced fast cameras, like the one whose measurements are discussed in this paper, can produce Gbytes of data per shot, the retrieval of the desired information can be quite demanding in terms of human resources.

In this paper, a series of algorithms are described for the exploitation of JET new fast visible camera (see section II). The aim is to develop automatic methods to recognize Multifaceted Asymmetric Radiation from the Edge instabilities (MARFEs) and Unidentified Flying Objects (UFOs) in video movies. UFOs are flakes released by JET first wall as a consequence of unusual power loads, typically due to instabilities like ELMs [2]. MARFE is a type of radiative instability that appears as an emissive region on the high field side in regimes of high plasma density [3].

The objective of the developed techniques of image processing is mainly exploratory: algorithms capable of detecting the event of interest, in this case UFOs and MARFEs, in an automatic way would be extremely useful. As a consequence, the first application of the techniques presented in the following consists of traversing JET database of images and identifying the frames with a high probability of containing signatures of MARFEs and/or UFOs. It is worth mentioning that the treatment in the rest of the paper is particularized for the case of JET wide angle fast visible camera only because it is the best instrument on JET to detect MARFEs and UFOs. On the other hand the developed algorithms are quite general and can therefore be applied to the images of other cameras. Indeed in the future it is planned to complement the information from JET fast camera with the analysis of InfraRed (IR) images as mentioned in section V.

With regard to the structure of the paper, next section is devoted to a brief description of JET fast visible camera. Section III describes the algorithms developed to identify MARFEs and reports on a statistical evaluation of their success rate. Section IV performs a similar analysis for the algorithms aimed at the detection of UFOs. The last section contains a short review of the techniques and outlines the directions of future investigations.

2. WIDE ANGLE FAST VISIBLE CAMERA

The results presented in this report are mainly based on the data recorded with one of the visible cameras that are installed on JET, the wide angle FAST visible camera. This camera is a Photron APX-RS which utilizes a CMOS detector [4]. The camera is installed on a Cassegrain endoscope, mainly devoted to an infrared view of JET first wall [5] but providing also a visible output. The wide field of view (70 degrees) of the system allows observing the divertor, the outer limiter, the upper limiter and the inner wall. In figure 1 the field of view of the visible wide angle camera, which is the same as the one of the IR camera, is shown.

The Photron APX-RS camera has a maximum frame size of 1024×1024 pixels at 3,000 frames per second, however the frame size can be reduced allowing faster capture up to 250,000 frames per second. The PNG output of the camera has been used as the input to Matlab to develop and run the algorithms described in this paper. Since in our application the information to be retrieved resides in the form of the objects detected by the camera, it is sufficient to analyse the luminosity of the various pixels and not special calibration, such as the one needed for IR thermography, has to be considered.

3. ALGORITHMS FOR THE DETECTION OF MARFES

Multifaceted asymmetric radiation from the edge phenomena, also referred to with the acronym MARFEs, are radiation condensation instabilities that appear in tokamaks as the density limit is approached. They are characterized by a small region where the radiative losses are higher than the input conducted power. They therefore consist of toroidally symmetric rings of enhanced radiation and usually occur on the high field side of the torus. MARFEs were firstly observed in the Alcator C Tokamak. In the frames of videos obtained with visible cameras, they appear as elongated regions of high emission as shown in the example of figure 2.

The detection of MARFEs by the analysis of the video available at JET is a very challenging proposition. In fact even if these events present clear features, their detection is not simple for the presence of noise in the videos, abrupt changes of the luminosity in the scene or high radiation in the divertor.

The developed MARFE detector is composed of two different blocks (fig.3). The Background Subtraction block performs a standard background subtraction [6], aimed at a first screening of the MARFE candidates. The Feature Analyser evaluates the spatial information and the evolution of the candidates and identifies those which have a high probability of being MARFEs. In the following subsections the details of these two bocks are provided.

3.1. MARFE BACKGROUND SUBTRACTION

One of the main problems in the identification of the MARFE candidates is the presence of many other events that present the same optical characteristics, such as flashes (probably caused by ELMs), high radiation of the plasma in the divertor or from the poloidal limiters. For this reason it is not easy to define a general approach that allows identifying and isolating clearly the MARFEs. The proposed approach is therefore based on a first preprocessing stage, consisting of standard Background subtraction; in this way it is possible to identify moving objects in the image.

Background subtraction techniques are in general based on the comparison of each frame with a reference or background model. Pixels in the current frame that are different from the background are considered to be moving objects (foreground). Obviously a successive processing stage is needed in order to localize and track the objects of interest. In our application, the choice of the background is a very important task. Several background modelling techniques have been presented in the literature [6]: the simplest approach is to consider the previous frame as the background. This approach is very useful for applications that need a fast adaptation to changes of the scene. Other techniques are based on the modelling of the background as a Gaussian distribution.

In our approach the averaging filter [7] is used in order to obtain the background model. This method evaluates the background as the mean of the previous *N* frames. This solution is very simple to implement and it has only a drawback: the high quantity of memory needed to store the previous *N* frames. The preliminary results show that with a number of frames of around 20 it is possible to achieve good performances. On the other hand, it is possible to use a recursive version of median filter, the approximate median filter [8], that does not need to store the *N* previous frames. In this scheme, the running estimate of the median (instead of the average) is incremented by one if the input pixel is larger than the estimate background, and decreased by one if smaller. This estimate eventually converges to a value for which half of the input pixels are larger than and half are smaller than the median. It is worth mentioning that the approximate median filter is well suited also for real time applications. In this case the approximate median filter provides better results of the average filter since it generates both less false positives and less false negatives.

When the background (*B*) is estimated, it is possible to compare it to the current frame (*I*) and identify objects in the foreground for each spatial location (*x,y*) (fig. 4). The simplest approach for foreground detection is to check whether the pixels of *I* are significantly different from the corresponding pixel of *B*. A threshold *T* is commonly used as shown below:

$$|I(x, y) - B(x, y)| > T \tag{1}$$

Another popular threshold system is presented in [9] and shown in equation (2), where the parameters μ_d and σ_d are respectively the mean and the standard deviation of *I(x,y)-B(x,y)*

$$|I(x, y) - B(x, y) - \mu_d| / \sigma_d > T \tag{2}$$

No great difference has been detected in the final success rate by adopting equation (1) or equation (2). Therefore, in the final solution of the algorithm the approximate median filter and equation (1) have been used to identify foreground objects; an example is shown in figure 5. In order to remove noise or artefacts introduced by the background subtraction phase, a control on the area of the identified objects is applied. For the results reported in this paper, it has been found that regions smaller than 70 pixels or bigger than 25% of the image can be safely rejected.

3.2. FEATURE ANALYZER

The background subtraction block detects every object that is on the foreground in the current frame. The aim of the Feature analyzer is to discriminate between objects that are signatures of MARFEs and objects that are due to other effects. In fact during the pulses, abrupt changes in the luminosity (for example after events like ELMs) or a higher radiation level in the divertor zone can lead to the presence of a new object in the foreground.

The Feature analyzer (FA) is mainly composed of two blocks as shown in figure 6.

The first block is used for the object tracking in successive frames. In this way it is possible to remove objects that are due to noise or in any case remain in the videos for an insufficient number of frames. This part of the algorithm is also aimed at identifying the objects which correspond to the same physical event but change position and/or shape in different frames.

The second block evaluates the motion of the objects, in order to recognize static objects such as hot spots. Moreover, also the objects that do not show characteristic MARFE movement (typically a vertical rigid movement) are discarded.

The object tracking algorithm is based on the evaluation of Statistical Moments for binary image analysis. As previously mentioned, the background subtraction step gives as output a binary image. One of the advantages of binary images is that they can be easily processed and analyzed. All the geometrical properties of the objects can be easily determined by means of statistical moments [10]. Moreover, with this tool it is possible to obtain information that are invariant to translation, rotation and scaling. The use of the statistical moments is crucial for this application, in which objects which can be in very different positions inside the field of view have to be identified.

By definition, given a bidimensional function *f(x,y),* it is possible to define a moment of grade *p+q* as follows:

$$M_{pq} = \int_{-\infty}^{+\infty}\int_{-\infty}^{+\infty} x^p y^q f(x, y)\,dxdy \tag{3}$$

For a binary image *I* it is possible to write a discrete form of equation (3):

$$m_{pq} = \sum_x \sum_y x^p y^q I(x, y) \tag{4}$$

As can be easily shown, the moment m_{00} represents the area of the binary object. Two additional

parameters that are very important in binary image processing are the barycentres. These parameters are obtained combining the first order moments and the m_{00} as in the following equation (5):

$$\bar{x} = \frac{m_{10}}{m_{00}}; \qquad \bar{y} = \frac{m_{01}}{m_{00}} \tag{5}$$

In figure 7 an example of identified MARFE (marked with red boundaries) and its barycentre (yellow cross) is shown.

The centralized normalized moments have been introduced by Hu [10] as m_{pq}:

$$\mu_{pq} = \sum_x \sum_y (x - \bar{x})^p (y - \bar{y})^q I(x, y) \tag{6}$$

These moments are essentially the same moments shown in equation 3, but are centralized and for this reason are invariant to translation.

Hu also introduced the moments η_{pq} that are scale invariant:

$$\begin{aligned} \eta_{pq} &= \frac{\mu_{pq}}{\mu_{00}^{\gamma}} \\ \gamma &= \frac{p+q}{2} + 1, \quad \forall (p+q) \geq 2 \end{aligned} \tag{7}$$

where .

The η_{pq} can be normalised with respect to changes in scale. Moreover, Hu [10] described a set of 7 moments, which are also rotation invariant. They are a set of nonlinear centralised moments that are translation, scale and rotation invariant; their mathematical expressions are reported in relations (8)-(14). This set is widely used in pattern recognition experiments to successfully identify various types of objects.

$$\varphi_1 = \eta_{20} + \eta_{02} \tag{8}$$

$$\varphi_2 = (\eta_{20} - \eta_{02})^2 + (4\eta_{11})^2 \tag{9}$$

$$\varphi_3 = (\eta_{30} - 3\eta_{12})^2 + (3\eta_{21} - \eta_{03})^2 \tag{10}$$

$$\varphi_4 = (\eta_{30} + \eta_{12})^2 + (\eta_{21} + \eta_{03})^2 \tag{11}$$

$$\begin{aligned} \varphi_5 = {} & (\eta_{30} - 3\eta_{12}) \cdot (\eta_{30} + \eta_{12}) \cdot \left[(\eta_{30} + \eta_{12})^2 - 3 \cdot (\eta_{21} + \eta_{03})^2 \right] + \\ & + (3\eta_{21} - \eta_{03}) \cdot (\eta_{21} + \eta_{03}) \cdot \left[3(\eta_{30} + \eta_{12})^2 - (\eta_{21} + \eta_{03})^2 \right] \end{aligned} \tag{12}$$

$$\varphi_6 = (\eta_{20} - \eta_{02}) \cdot [(\eta_{30} + \eta_{12})^2 - (\eta_{21} + \eta_{03})^2] + 4\eta_{11}(\eta_{30} + \eta_{12}) \cdot (\eta_{21} + \eta_{03}) \quad (13)$$

$$\varphi_7 = (3\eta_{21} - \eta_{03}) \cdot (\eta_{30} + \eta_{12}) \cdot [(\eta_{30} + \eta_{12})^2 - 3 \cdot (\eta_{21} + \eta_{03})^2] + (\eta_{30} - 3\eta_{12}) \cdot (\eta_{21} + \eta_{03}) \cdot [3(\eta_{30} + \eta_{12})^2 - (\eta_{21} + \eta_{03})^2] \quad (14)$$

Another important parameter used in the proposed algorithm is the centre of the bounding box. For each object it is possible to define a minimum rectangle that encloses it: the bounding box. The centre of the bounding box is in general different from the barycentre of the object. In figure 8 an example of bounding box is shown.

In the following we refer to the object barycentre and bounding box centre as the object centroids.

To summarise, the main goal of the Object Tracking block consists of the identification of the objects in successive frames. Two main assumptions have to be satisfied in order to apply successfully this part of the algorithm. First of all, the acquisition rate of the camera must be sufficiently greater than the velocity of the objects so that they do not move too much between frames. Moreover, it is supposed that the background subtraction stage gives a good estimation of the foreground objects.

The binary images that contain the foreground objects are analyzed. For each object the features extracted are the object centroids ,and the Hu moments φ_i, i=1,…7.

Once the features of each object are calculated, a second feature analysis phase is needed. In particular, a control on two successive frames is applied in order to discriminate new objects in the videos from those that are still present on it. For each object in the frame *n*, several metrics are evaluated in order to estimate its distance from all the other objects in the frame *n*-1: the distance of the barycentres d_b, the distance between the centres of the bounding boxes d_c, the distance between the Hu moments d_φ. The closest object in the previous frame is chosen as the reference of the current object if the distance is reasonably small, in general lower than a predefined threshold (see appendix A for the details). If an object does not respect the previous criteria, it will be considered as a new object, otherwise it will be recorded as a known object (see figure 9).

Moreover, in order to remove some noise artefacts, an object is selected as a MARFE candidate only if it appears in the video more than a minimum number of frames N_m (see Appendix A).

The last step, in the evaluation whether an object can be considered a MARFE, consists of the analysis of its motion properties. For a given object, the Motion Estimation block is based on the analysis of the positions of its centroids in successive frames. In particular, an object is considered a MARFE candidate if three different conditions are verified at the same time (fig.10). First of all, the distance between the object centroids in successive frames is greater than a given threshold. The second condition requires that the motion component of centroids along the *y* axis is greater then the component along *x*. Finally, a control on the trajectory is performed. In particular, an

object is considered in motion as long as the y coordinate of its centroids decreases or increases for at least N_m frames.

The numerical values for these conditions, as implemented in the version of the algorithm described in this paper, are reported in Appendix A.

Summarising, the algorithm depends on 12 basic adjustable parameters, which are described in detail in [11]. An optimization process has been undertaken to identify the most suitable values of these parameters for the application at hand.

To test the performance of the algorithm, a set of 18 videos has been selected. About half of them contain clear signatures of MARFE instabilities and half of them do not. They have been carefully selected to cover a realistic and broad range of MARFE phenomenology in JET videos of the fast camera. They therefore present an average level of difficulty and they have not been intentionally biased to favor any specific situation. It is worth mentioning that, since JET fast visible camera can generate tens of thousand of frames per shot, the manual selection process is a very delicate and time consuming activity. The results in terms of success rates and false detections are provided in chart I. The fact that the algorithm manages to correctly identify more than 80% of the videos with a MARFE is certainly very encouraging and indeed it is planned to use this tool for a systematic data screening of JET database.

4. UFO DETECTION SYSTEM

The detection of UFOs requires a quite different procedure to obtain acceptable results. Indeed UFOs are much smaller objects, which typically appear approximately spherical in the frames of JET fast visible camera. Indeed, given the optical resolution of the endoscope it is not possible to resolve many details of tiny objects like UFOs. Moreover, UFOs can present morphological characteristics very similar to hot spots, regions of the vacuum vessel reaching high temperatures due to concentrated plasma-wall interactions. These hot spots are normally quite static on the time scale of the frame rate of JET fast camera and therefore they can be discriminated more on the basis of their movement than their shape.

In any case the developed UFO Detection System (UDS) system can be conveniently described as a combination of two main blocks, as shown in figure 11. The Single Frame UFO Detector (SFUD) is based on typical image processing algorithms and it is able to identify events that present patterns characteristic of UFOs. Unfortunately, as already mentioned, hot spots in the vacuum vessel, noise in the measurements or simply a variation of the luminance in the entire scene could generate patterns very similar to the ones of the UFOs. To avoid false detection (false positives), a Dynamic UFO Detector (DUD) is therefore required. By analysing the evolution of the identified UFO in successive frames, it is possible to eliminate static objects such as hotspots, particular high intensity regions or noisy objects and identify the UFOs.

4.1. UFO FEATURES AND FRAME PRE-PROCESSING

In the videos of JET wide angle fast camera, UFOs appear as bright small particles moving fast inside the vessel (see figure 12). Their detection will be based essentially on an algorithm that is able to detect the intensity level variations.

The complexity of the application could in principle be reduced by using different pre-processing techniques. In fact images with a high contrast are more suitable for the UFO identification. We have tried several image enhancement algorithms, such as histogram equalization, intensity pixel transformation [12] etc. but the results obtained have not been very satisfactory. The main problem is to adapt the algorithm parameters to each frame; indeed, during a discharge, the grey level intensity of the entire scene can change significantly. Moreover, these characteristics vary also between different pulses. Therefore the decision has been made to process the frames by the algorithm without any pre-processing except for the grey level transformation.

4.2. SINGLE FRAME UFO DETECTOR

The complete scheme of the Single frame UFO Detector (SFUD) is shown in figure 13. It consists of a first stage aimed at extracting the objects (called details extraction) present in the image, followed by an edge detector and an edge linking steps. The final area thresholding is meant to eliminate all the objects which do not have an area compatible with UFOs. All these steps are described in detail in the following.

4.2.1 Details extraction

As previously mentioned, the main idea of the algorithm is the detection of the variations in the pixel intensity. It means that we need to extract the high frequency components of the image. The simplest approach would be to apply a high pass filter or a band pass filter in order to obtain also noise reduction at the low frequencies. The problem with these filters is to tune the filter parameters in the right way. As for the pre-processing algorithms, each frame or different videos need different parameters in order to obtain good results. For this reason we use a different approach to extract the details of the image, which does not make recourse to any absolute value of the emission in the images. As shown in figure 14, the high frequency image is obtained subtracting a blurred version of the image from the original one. In particular a classical average filter is used in order to obtain the smoothed (or blurred) version of the image. The only parameter that has to be tuned is the filter dimension but this does not strongly influence the algorithm performances. A filter dimension of 10 seems to work satisfactorily for the videos analyzed.

4.2.2. Edge detection

The frame derived the previous step is then scanned by a classical edge detector algorithm. A threshold system is applied on the resulting image. The binary image obtained contains all the information about all the significant variations of the intensity. Although a similar result could be

achieved applying an edge detector algorithm to the original frame, our proposed approach is less sensitive to the noise.

In more detail, the edge detection algorithm used is the Laplacian filter; but Sobel, Prewitt filter or the Canny algorithm could be used as well [12]. The results of Sobel and Prewitt mask are more sensitive to the threshold value; the Canny algorithm gives the best results, but it has a higher computational complexity [12]. The Laplacian filter gives the best trade-off between results and computational costs. In figure 15 an example of a frame with UFOs and hot spots and the detected edges is shown. As can be easily noticed, the algorithm detects every edge including for example the boundary of the divertor region. Obviously these elements are not UFOs and they can be easily discarded as UFO candidates on the basis of their shape and area.

4.2.3.Edge Linking

Theoretically edge detection algorithms should identify only the pixels lying on the edges of the objects to be identified. In many practical cases however a lot of spurious discontinuities in the intensity values are present in the image resulting from the edge detection stage. Therefore the edge detection stage is usually followed by edge linking algorithms, to group edge pixels into meaningful edges. In the literature several methods are described to perform this step. In the proposed approach we apply a technique very suited to the manipulation of binary images (as the ones that are the result of the Edge detection block): the morphological operators [12].

Morphological Image Processing is a category of very powerful tools to extract image components like: boundaries, skeletons etc., but these techniques are used also for thinning, filtering and pruning. In our application we use these techniques to fill the gap in the edge and fill the holes in the binary images. As shown in figure 15, some of the UFOs are not completely enclosed by an edge. The main idea is to apply morphological operators in order to complete these gaps.

Some morphological operators have been used in our algorithm to complete the edges. To fill gap and discontinuities, the dilation operator has been used [12]. This operator “grows” objects in binary images. It is possible to tune the growth choosing the size of the operator and its shape. Typically the objects are dilated by the dilatation operator; by changing the shape of the operator it is possible to obtain different results. Another simple operator that we have used in the developed algorithm is the erosion operator [12]. This operation “shrinks” or “thins” objects in a binary image. This operator is usually adopted to refine the contours of objects. In many applications it works as a filter, in fact it removes small artefacts attached to edges and contours of bigger objects.

These morphological operations can be applied in different ways, tuning their size for example. Moreover, different combinations of them could lead to different results. A quite good combination of the previous operations is a three step process obtained by a dilation stage to fill the gaps, an erosion stage with a small operator in order to remove noise introduced by the previous step and a filling procedure to obtain objects in the binary image. An example of the results of this process is shown in figure 16.

5. AREA THRESHOLDING

The image obtained in the previous section is a binary image that contains all the objects highlighted by the morphological operators. As it is clearly seen in figure 16, also the boundaries of the divertor and of the inner wall of the vacuum vessel have been retained in the image even if they are not UFOs. Also some little spots, that probably represent noise, are present in the processed image. With a simple threshold on the area of the objects, it is possible to eliminate these undesired objects. The result of the area thresholding is shown in figure 17; in this case regions with an area smaller than 3 pixels or bigger than 35 pixels have been rejected as unrealistic candidates for UFOs. As we can see in figure 18, where the boundaries of the detected objects have been superimposed on the original image, there are still some objects which have been retained but do not represent UFOs particularly in the bottom left part of the frame. On the other hand, these undesired objects have the same morphological characteristics as the UFOs and therefore they cannot be discriminated at the level of static analysis of individual frames. These false positives can be avoided only making recourse to dynamic detection, i.e. a dynamic UFO Detector. A Dynamic UFO Detector (DUD) would analyze successive binary frames obtained with the SUFD; the goal of this stage would be the tracking of objects that move in the image and the recognition of objects that are fixed or changing their shape and position at a rate too slow to be due to UFOs. On the other hand, a dynamic analysis of UFOs is particularly difficult. In addition to the high number of objects to be identified and whose movement is to be followed, the trajectories are very complex. They can intersect, be occluded by structures in the field of view or simply present discontinuities due to changes in emission. Therefore the development of a robust dynamic UFO detector will be the subject of a future activity. In any case it has been possible to make a preliminary assessment of the detection capability of the present identifier because the detection of UFOs by the fast camera is a very rare event. Therefore the main danger would be false alarms. To assess this issue, a video with UFOs has been analysed together with 100 videos without any UFOs and the algorithm has managed to successfully identify the video with the UFOs without any false alarm.

To summarise this section, an UFO detection algorithm has been developed and the preliminary results are very promising. The static algorithm is quite robust in detecting UFOs and is not too vulnerable to false alarms. With a second stage, analyzing successive frames, it is expected that the success rate in the detection will be satisfactory. On the other hand, given the complexity of the UFO trajectories in JET videos, in order to develop such a dynamic detector a higher statistics of examples will be required.

CONCLUSIONS

This paper describes the development of image processing algorithms for the automatic identification of MARFEs and UFOs in JET cameras. The main aim of the work has been to converge on algorithms good enough to perform a first exploratory phase, to identify frames with similar events in JET database. This is required since a specific database of images with MARFEs or UFOs is not available

in JET. The first results of this exploratory phase are quite encouraging. In the case of MARFEs, the algorithms developed manage to identify the presence of MARFE signatures in the videos with a success rate of more than 80 %. In the case of UFOs not enough events have been captured so far by the camera to allow a comparable statistics On the other hand, in the few cases available, the devised algorithms manage to properly discriminate the UFOs from the other objects present in the frames. In this respect, a dynamic analysis, comparing different frames, has proved necessary to distinguish UFOs from hot spots, which can have very similar visual characteristics.

With regard to future developments, first of all, after more examples have been retrieved from JET database of videos, the algorithms will have probably to be further refined and optimised. Another line of activity will involve JET IR cameras. In some cases both MARFE and UFOs are detected also in the IR range. The algorithms will certainly have to be modified to identify efficiently the objects also in the IR videos. A different line of activities involves control applications. For both machine protection and disruption prediction, it would be very useful to be able to detect MARFEs and UFOs in real time. The requirements in term of both accuracy and computational time are under revision particularly in the context of the operation of JET with the new ITER-like wall.

ACKNOWLEDGMENTS

This work, supported by the European Communities under the contract of Association between EURATOM and ENEA and EURATOM and CEA, was carried out under the framework of the European Fusion Development Agreement. The views and opinions expressed herein do not necessarily reflect those of the European Commission.

REFERENCES

[1]. A. Murari *et al*., Plasma Phys. Control. Fusion **50** (2008) 124043 (12pp)

[2]. ASDEX Team, Nuclear Fusion **29**, 1959 (1989)

[3]. B. Lipschultz, J. Nucl. Mater. 145-147 (1987) 15

[4]. J A Alonso *et al*. 2007 *Proc. 34th EPS conf. on Control. Fusion and Plasma Physics (Warsaw, Poland)*

[5]. E. Gauthier *et al* Fusion Engineering and Design, **82**(5-14):1335-1340, 2007

[6]. Piccardi, M. Man and Cybernetics, 2004 IEEE International Conference on vol. 4, Issue , 10-13 Oct. 2004 Page(s): **3099** – 3104.

[7]. R. Cucchiara, M. Piccardi, and A. Prati, IEEE Transactions on Pattern Analysis and Machine Intelligence **25**, pp. 1337–1342, Oct 2003.

[8]. N. McFarlane and C. Schofield, Machine Vision and Applications 8(3), pp. 187–193, 1995.

[9]. S.S Cheung and C. Kamath, Robust background subtraction with foreground validation for urban traffic video. EURASIP J. Appl. Signal Process. 2005

[10]. M. K. Hu, IRE Trans. Info. Theory, vol. IT-8, pp.**179–187**, 1962.

[11]. F. Delaunay, M. Camplani, A. Murari and D. Mazon "*First attempts to automatically detect MARFEs in JET videos*" JET technical report

[12]. Rafael C. Gonzalez and Richard E. Woods. Digital Image Processing. Addison-Wesley Longman Publishing Co., Inc., Boston, MA, USA, 2001.

APPENDIX A.

Summary of the adjustable parameters of the code implementing the algorithm for the MARFE detection.

The following list includes all the adjustable parameters of the code implementing the algorithm for the MARFE detection, with their meaning and their influence in the process of detection.

Background subtraction parameters

- size of the frame buffer N.
- threshold T for foreground estimation.
- object tracking parameters
- threshold T_φ on the distance d_φ in the 7-dimensional space of the Hu moments.
- threshold T_b on the distance d_b between the barycenters.
- threshold T_c on the distance d_c between the centers of the bounding boxes.
- minimum number of frames N_m

Motion estimation

- threshold T_b on the distance d_b between the barycenters
- threshold T_c on the distance d_c between the centers of the bounding boxes.
- threshold T_{bx}(T_{by}) on the distance on x (y) axis between the barycenters
- threshold T_{cx}(T_{cy}) on the distance on x (y) axis between the bounding boxes.

The values of these parameters used to obtain the results described in this paper are:

- $N = 20$
- $T = 15$
- $T_b = 7$
- $T_c = 6$
- $T_\varphi = 0.25$
- $T_b = T_c = 10$
- $T_{bx} = T_{cx} = 7$
- $T_{by} = T_{cy} = 8$
- $N_m = 3$

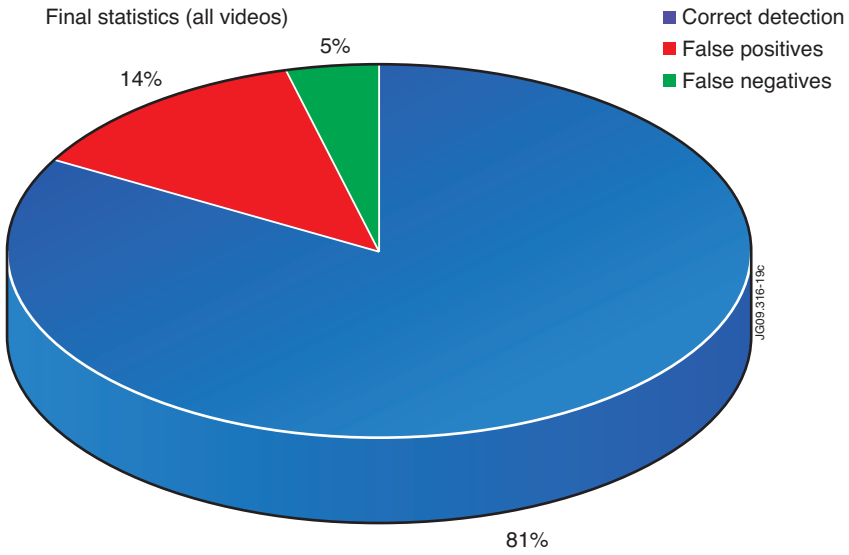

Chart I: Percentages of correct detections, false positives and false negatives of the optimised version of the algorithm for the identification of MARFEs

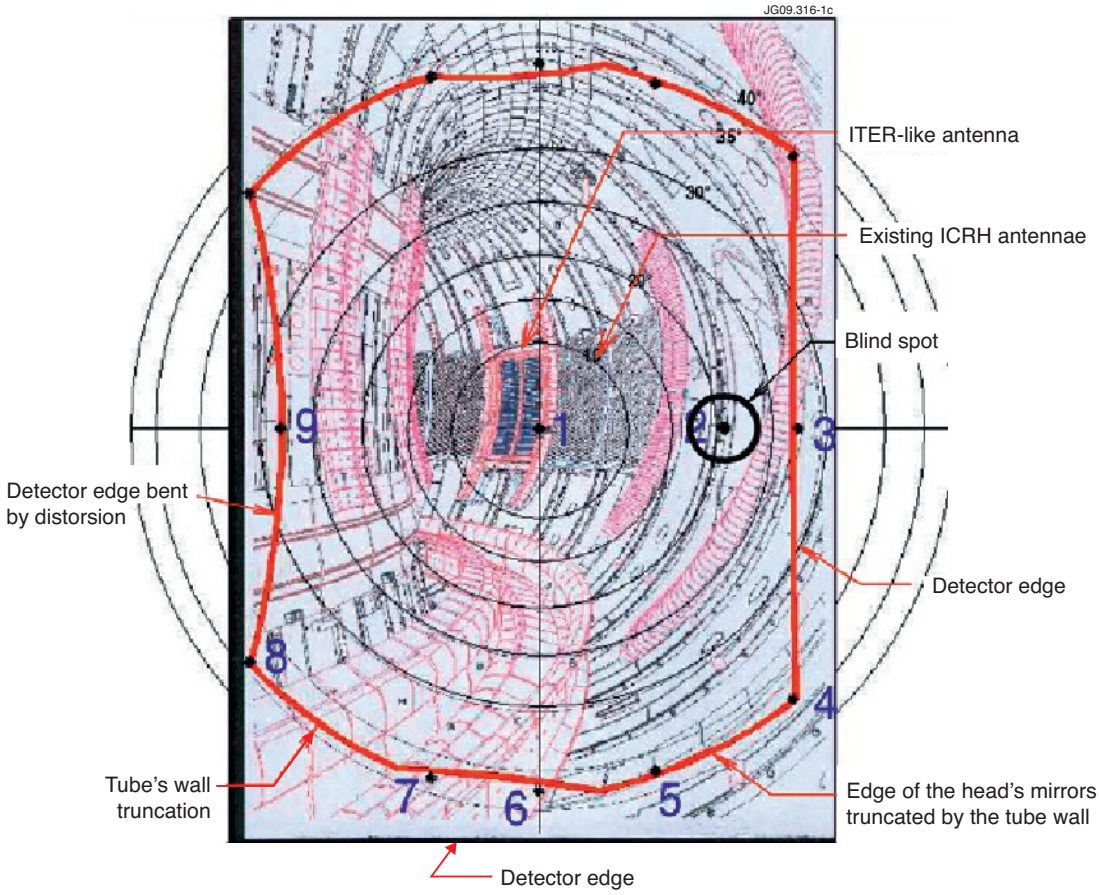

Figure 1: Field of view of the wide angle fast visible camera of JET.

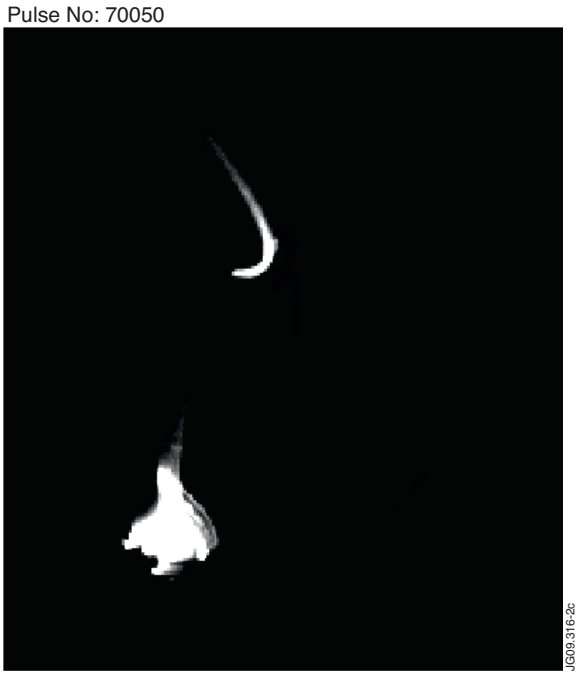

Figure 2: Example of MARFE.

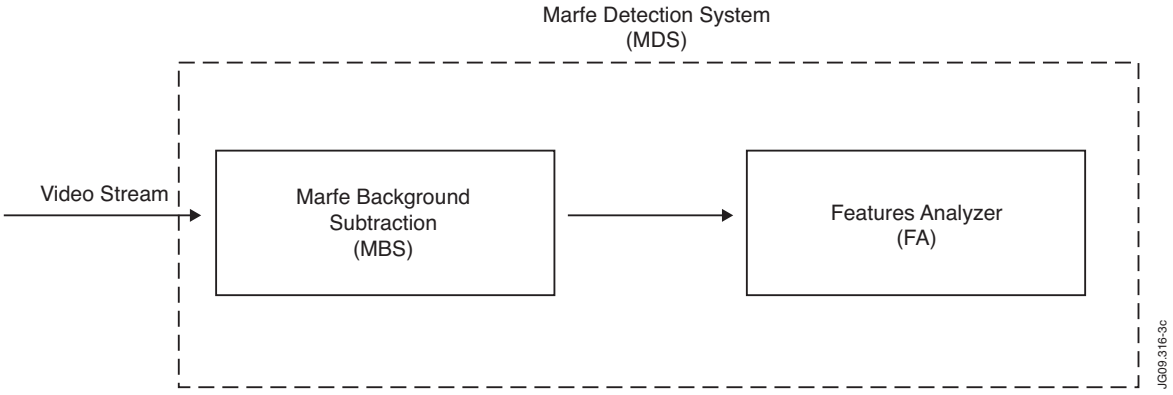

Figure 3: MARFE Detection System (MDS) .

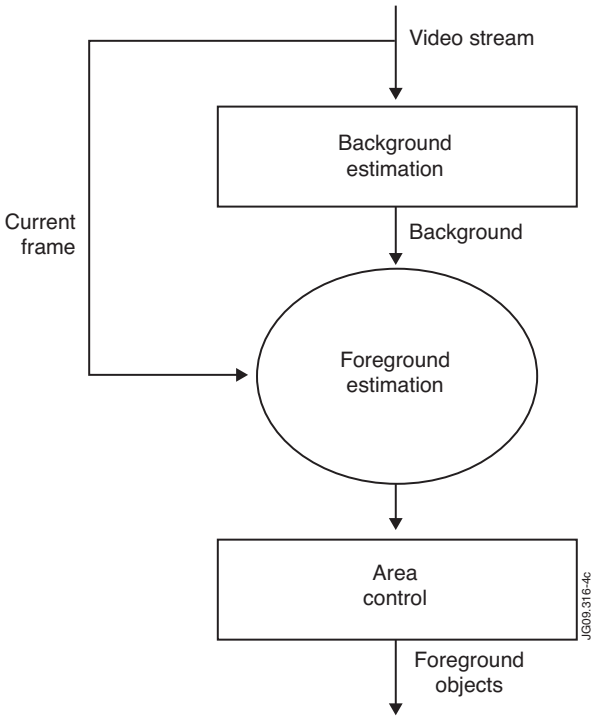

Figure 4: Block diagram of the MARFE background subtraction procedure.

Figure 5: Example of detected MARFE.

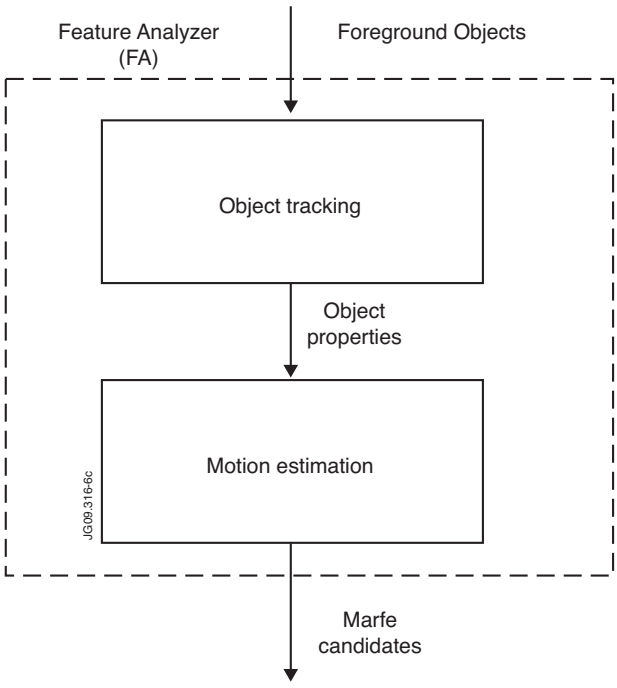

Figure 6: Block diagram of the Feature Analyzer.

Figure 7: Example of the barycentre for a detected MARFE.

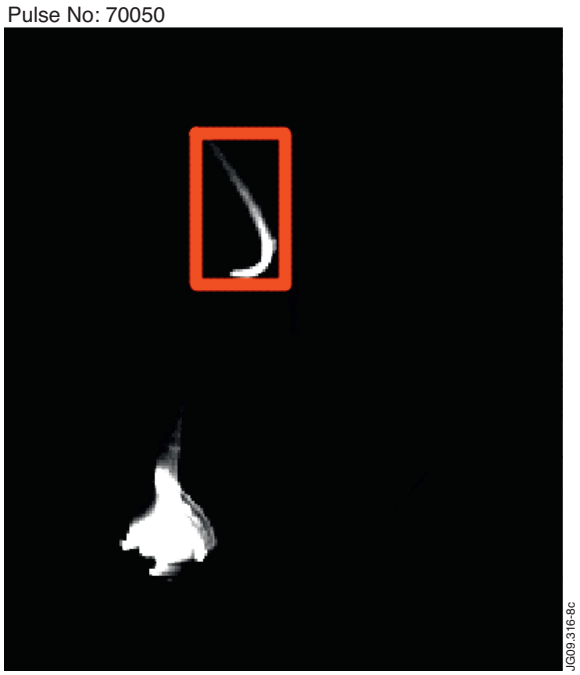

Figure 8: Example of bounding box for a detected MARFE.

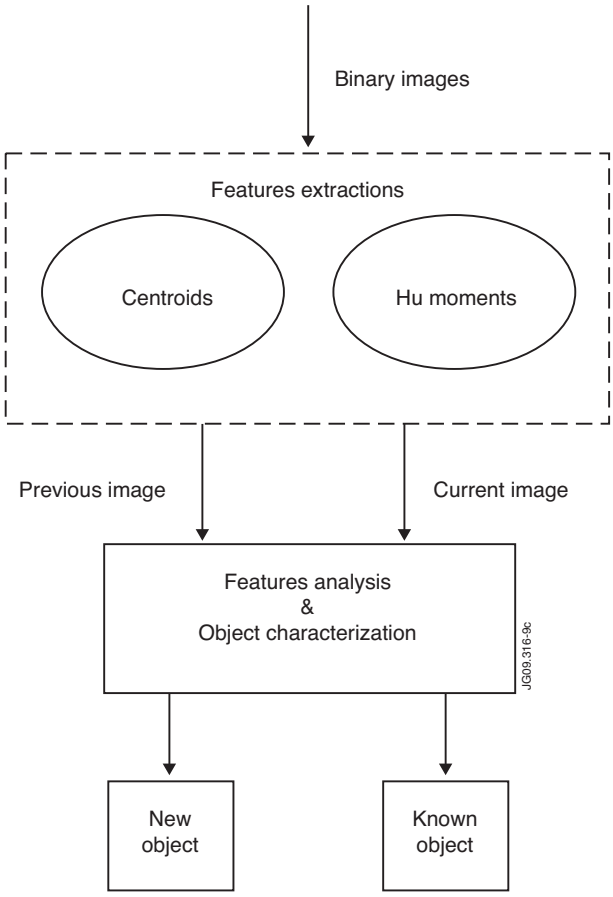

Figure 9: Object tracking block.

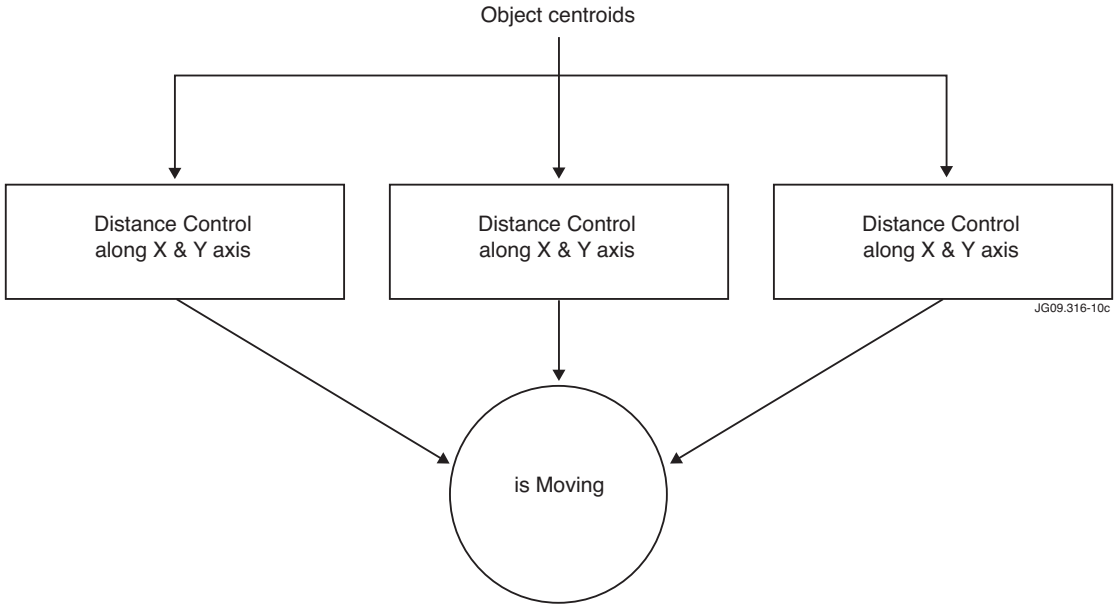

Figure 10: Motion Detection block: the various conditions on the motion of an object to determine whether it is a good MARFE candidate.

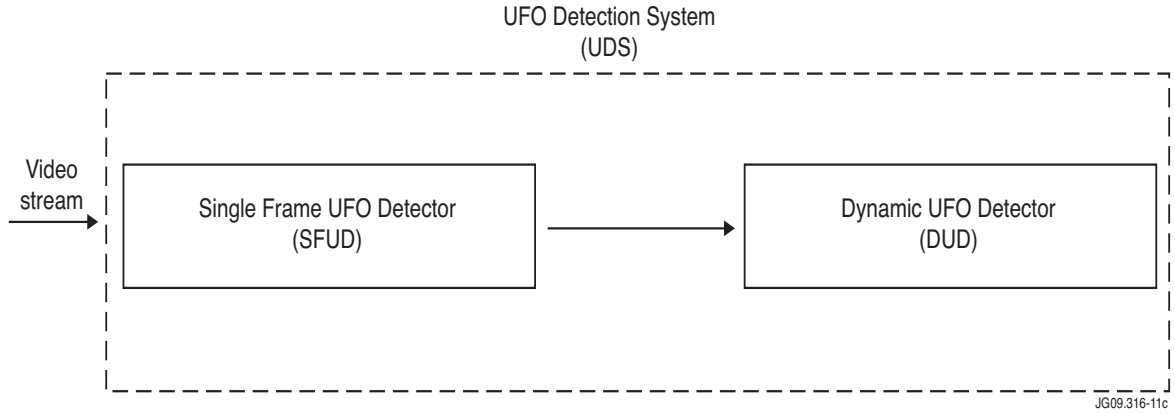

Figure 11: UFO Detection system (UDS) block diagram.

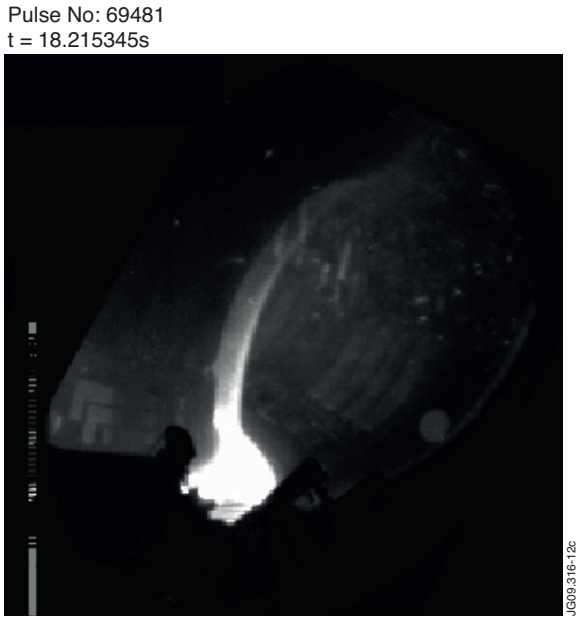

Figure 12: An example of UFO Pulse No: 69481. The UFOs appear manly in the top right part of the image.

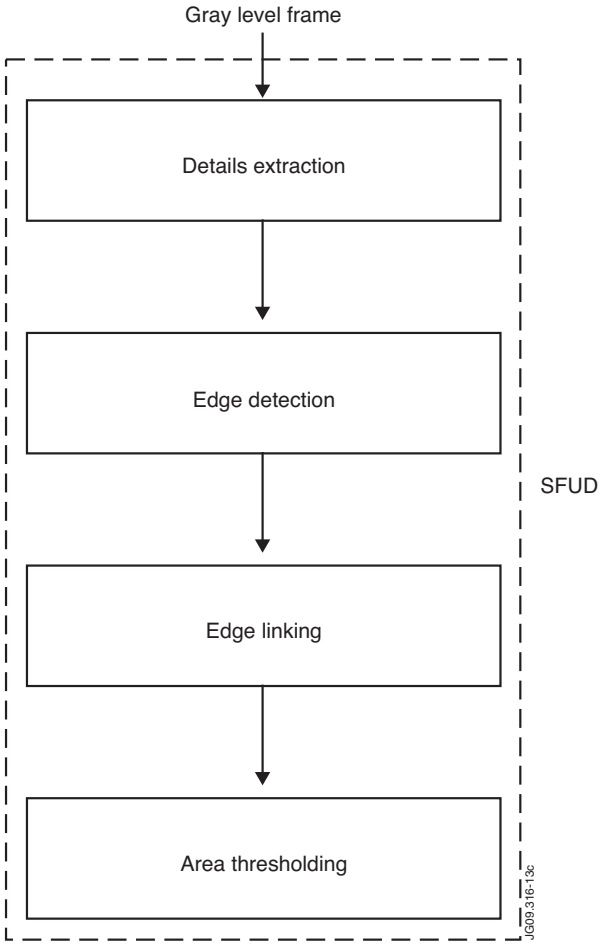

Figure 13: Single frame Detectorscheme.

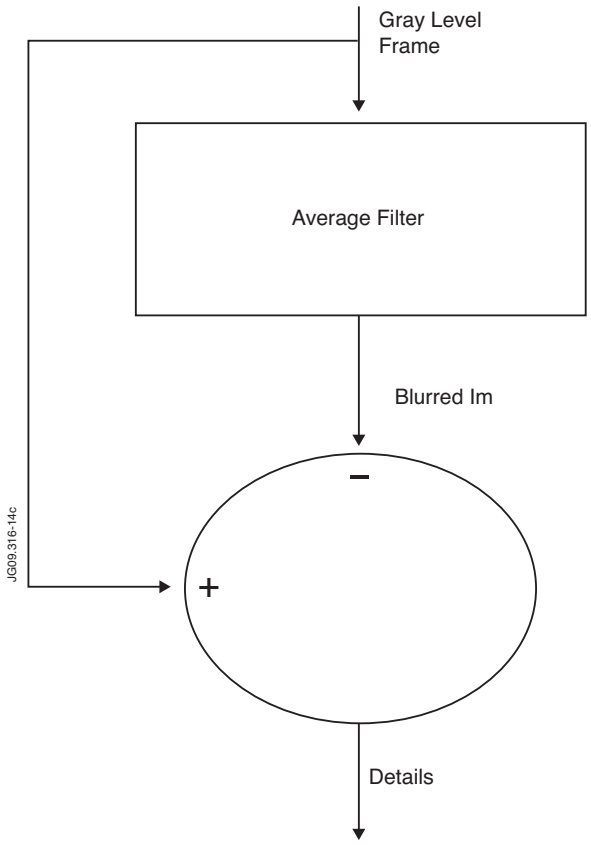

Figure 14: Details Extraction Block.

Figure 15: Example of Edge Detection Stage.

Figure 16: Binary image obtained after the application of the morphological operators.

Figure 17: Objects retained in the image after the area thresholding step.

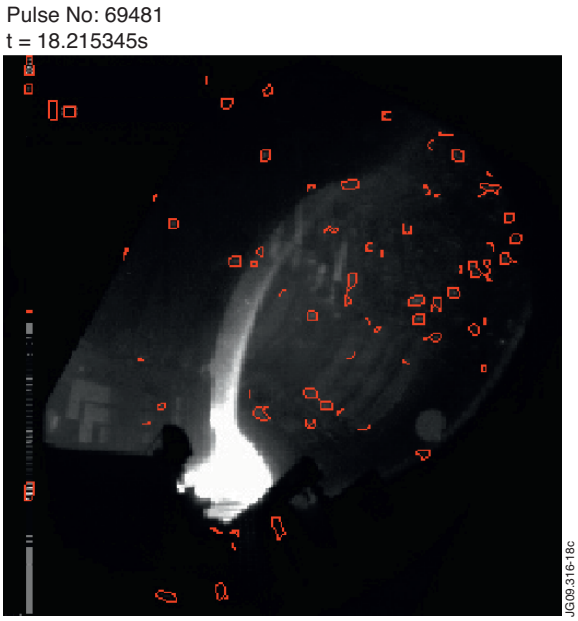

Figure 18: Boundaries of the objects identified by the static UFO detector overlapped onto the original image.